*Inorg. Chem.* **2003**, *42*, 2742–2750

# Two New Groups of Homoleptic Rare Earth Pyridylbenzimidazolates: $(NC_{12}H_8(NH)_2)[Ln(N_3C_{12}H_8)_4]$ with Ln = Y, Tb, Yb, and $[Ln(N_3C_{12}H_8)_2(N_3C_{12}H_9)_2][Ln(N_3C_{12}H_8)_4](N_3C_{12}H_9)_2$ with Ln = La, Sm, Eu

**Klaus Müller-Buschbaum* and Catharina C. Quitmann**

*Institut für Anorganische Chemie, Universität zu Köln, Greinstrasse 6, D-50939 Köln, Germany*

Received November 20, 2002

The compounds $(NC_{12}H_8(NH)_2)[Ln(N_3C_{12}H_8)_4]$, Ln = Y, Tb, Yb, and $[Ln(N_3C_{12}H_8)_2(N_3C_{12}H_9)_2][Ln(N_3C_{12}H_8)_4](N_3C_{12}H_9)_2$, with Ln = La, Sm, Eu, were obtained by reactions of the group 3 metals yttrium and lanthanum as well as the lanthanides europium, samarium, terbium, and ytterbium with 2-(2-pyridyl)-benzimidazole. The reactions were carried out in melts of the amine without any solvent and led to two new groups of homoleptic rare earth pyridylbenzimidazolates. The trivalent rare earth atoms have an eightfold nitrogen coordination of four chelating pyridylbenzimidazolates giving an ionic structure with either pyridylbenzimidazolium or $[Ln(N_3C_{12}H_8)_2(N_3C_{12}H_9)_2]^+$ counterions. With Y, Eu, Sm, and Yb, single crystals were obtained whereas the La- and Tb-containing compounds were identified by powder methods. The products were investigated by X-ray single crystal or powder diffraction and MIR and far-IR spectroscopy, and with DTA/TG regarding their thermal behavior. They are another good proof of the value of solid-state reaction methods for the formation of homoleptic pnicogenides of the lanthanides. Despite their difference in the chemical formula, both types $(NC_{12}H_8(NH)_2)[Ln(N_3C_{12}H_8)_4]$, Ln = Y (**1**), Tb (**2**), Yb (**3**), and $[Ln(N_3C_{12}H_8)_2(N_3C_{12}H_9)_2][Ln(N_3C_{12}H_8)_4](N_3C_{12}H_9)_2$, Ln = La (**4**), Sm (**5**), Eu (**6**), crystallize isotypic in the tetragonal space group $I4_1$. Crystal data for (**1**): $T = 170(2)$ K, $a = 1684.9(1)$ pm, $c = 3735.0(3)$ pm, $V = 10603.5(14) \times 10^6$ pm$^3$, R1 for $F_o > 4\sigma(F_o) = 0.053$, wR2 = 0.113. Crystal data for (**3**): $T = 170(2)$ K, $a = 1683.03(7)$ pm, $c = 3724.3(2)$ pm, $V = 10549.4(14) \times 10^6$ pm$^3$, R1 for $F_o > 4\sigma(F_o) = 0.047$, wR2 = 0.129. Crystal data for (**5**): $T = 103(2)$ K, $a = 1690.1(2)$ pm, $c = 3759.5(4)$ pm, $V = 10739(2) \times 10^6$ pm$^3$, R1 for $F_o > 4\sigma(F_o) = 0.050$, wR2 = 0.117. Crystal data for (**6**): $T = 170(2)$ K, $a = 1685.89(9)$ pm, $c = 3760.0(3)$ pm, $V = 10686.9(11) \times 10^6$ pm$^3$, R1 for $F_o > 4\sigma(F_o) = 0.060$, wR2 = 0.144.

## Introduction

Homoleptic amides of the lanthanides as well as of group 3 metals are still rarely found in the literature. Contrary to this, there has been major interest in the study of silyl amides of the lanthanides including homoleptic species.[1−3] Of homoleptic non-silyl amides, sandwich porphyrinogen complexes have been investigated intensively,[4−6] including the reductive potential of the chelated lanthanide.[7−9] Homoleptic pyrazolates were another field of study,[10,11] also in the context of metal based reactions. Other examples such as bis(1-alkylbenzimidazole)2-yl-pyridine complexes are known to form homoleptic species only in the presence of weakly coordinating units such as the perchlorate anion.[12] In a previous study,

* To whom correspondence should be addressed. E-mail: Klaus.Mueller-Buschbaum@uni-koeln.de. Fax: 0049 221 470 5083.

(1) Arndt, S.; Okuda, J. *Chem. Rev.* **2002**, *102*, 1953−1976.
(2) Kempe, R.; Noss, H.; Irrgang, T. *J. Organomet. Chem.* **2002**, *647*, 12−20.
(3) Schumann, H.; Meese-Marktscheffel, J. A.; Esser, L. *Chem. Rev.* **1995**, *95*, 865−986.
(4) Darovsky, A.; Wu, L. Y.; Lee, P.; Sheu, H. S. *Acta Crystallogr.* **1991**, *C47*, 1836−1838.
(5) Haghighi, M. S.; Teske, C. L.; Homborg, H. *Z. Anorg. Allg. Chem.* **1992**, *608*, 73−80.
(6) De Cian, A.; Moussavi, M.; Fischer, J.; Weiss, R. *Inorg. Chem.* **1985**, *24*, 3162−3167.
(7) Evans, W. J. *Coord. Chem. Rev.* **2000**, 263−283.
(8) Campazzi, E.; Solari, E.; Floriani, C.; Scopelliti, R. *J. Chem Soc., Chem. Commun.* **1998**, 2603−2604.
(9) Dube, T.; Gambarotta, S.; Yap, G. P. A. *Angew. Chem., Int. Ed.* **1999**, *38*, 1432−1435; *Angew. Chem.* **1999**, *111*, 1507−1510.
(10) Pfeiffer, D.; Ximba, B. J.; Liable-Sands, L. M.; Rheingold, A. L.; Heeg, M. J.; Coleman, D. M.; Schlegel, H. B.; Kuech, T. F.; Winter, C. H. *Inorg. Chem.* **1999**, *38*, 4539−4548.
(11) Deacon, G. B.; Forsyth, C. M.; Nickel, S. *J. Organomet. Chem.* **2002**, *647*, 50−60.
(12) Piguet, C.; Williams, A. F.; Bernardinelli, G.; Bünzli, J.-C. G. *Inorg. Chem.* **1993**, *32*, 4139−4149.



10.1021/ic020681u CCC: $25.00 
Published on Web 03/27/2003

**Chart 1.** 2-(2-Pyridyl)-benzimidazole

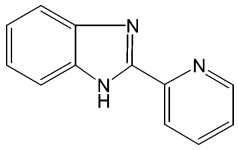

we presented homoleptic lanthanide ammonium salts with 2-(2-pyridyl)-benzimidazole as the first examples of lanthanide pyridylbenzimidazolates.[13] In this work, we present two new groups of homoleptic pyridylbenzimidazolates of the lanthanides and of group 3 metals. Furthermore, it is shown that the new compounds presented are formed in reactions of the lanthanide metals with molten 2-(2-pyridyl)-benzimidazole (Chart 1) at lower temperatures whereas the ammonium salts presented before are thermal decomposition products at higher temperatures, thus resulting from compounds similar to the two new homoleptic types.

## Experimental Section

**General Data.** All manipulations were carried out under inert atmospheric conditions using glovebox, ampule, as well as vacuum line techniques. Heating furnaces with $Al_2O_3$ tubes together with Eurotherm 2416 control elements were used for the ampule experiments. The IR spectra were recorded using a Bruker FTIR-IS66V-S spectrometer, the Raman spectra, using a Bruker FRA 106-S spectrometer. For MIR investigations, KBr pellets, and PE pellets for far-IR, were used under vacuum. The thermal decompositions of **(1**−**6)** were studied using simultaneous DTA/TG (Netzsch STA-409). A 34.0 mg amount of the bulk of the Y reaction **(1)**, 12.0 mg for Tb **(2)**, 14.8 mg for Yb **(3)**, 17.5 mg for La **(4)**, 9.8 mg for Sm **(5)**, and 9.3 mg of the Eu **(6)** reaction were heated from 293 K up to 1073 K at a heating rate of 10 K/min in a constant Ar flow of 60 mL/min.

**$(NC_{12}H_8(NH)_2)[Y(N_3C_{12}H_8)_4]$ (1).** Y (1 mmol = 89 mg) and 2-(2-pyridyl)-benzimidazole (2 mmol = 390 mg) together with Hg (0.125 mmol = 25 mg) were sealed in an evacuated Duran glass ampule and heated to 300 °C in 5 h. The reaction mixture was then cooled to 250 °C over 172 h and down to 130 °C in 100 h. It was then cooled to room temperature within 24 h. Except for some Hg and excess Y, the reaction mixture showed white milky crystals of the product, which is air and moisture sensitive. Anal. Calcd $C_{60}H_{42}N_{15}Y$: C, 67.95; N, 19.81; H, 3.96. Found: C, 68.04; N, 20.00; H, 4.18. MIR (KBr): 3080 w, 3040 m, 2923 w, 2853 w, 1600 s, 1565 m, 1509 m, 1473 m, 1454 s, 1440 s, 1421 vs, 1373 s, 1329 s, 1294 m, 1278 s, 1250 m, 1147 m, 1117 w, 1094 w, 1051 w, 1006 m, 978 m, 820 m, 803 m, 745 vs, 645 m $cm^{-1}$. Far-IR (PE): 542 w, 474 w, 414 vw, 243 w, 232 w, 194 w, 73 w $cm^{-1}$. DTA/TG (Ar): 350 °C, calcd $M(NH_4[Y(N_3C_{12}H_8)_4])$ = 83.3% of $M((NC_{12}H_8(NH)_2)[YN_3C_{12}H_8)_4]$; measured, 84%; 430 °C, calcd M(C,Y) = 72.6% of $M(NH_4[Y(N_3C_{12}H_8)_4])$; measured, 75%.

**$(NC_{12}H_8(NH)_2)[Tb(N_3C_{12}H_8)_4]$ (2).** Tb (1 mmol = 159 mg) and 2-(2-pyridyl)-benzimidazole (1 mmol = 195 mg) together with Hg (0.25 mmol = 50 mg) were sealed in an evacuated Duran glass ampule and heated to 250 °C in 2.5 h. The reaction mixture was heated further to 270 °C over 1 h and the temperature held for 288 h. The reaction mixture was then heated to 300 °C in 6 h and the temperature held within 72 h. It was then cooled to 200 °C over 200 h and to room temperature in another 20 h. Except for some Hg and unreacted material, the reaction mixture showed a badly crystalline yellow product, which is air and moisture sensitive. MIR (KBr): 3078 w, 3047 m, 1600 vs, 1565 m, 1507 s, 1472 m, 1441 vs, 1421 vs, 1370 s, 1327 s, 1295 m, 1270 s, 1251 m, 1150 m, 1119 w, 1095 w, 1050 w, 1007 m, 975 m, 905 m 815 m, 796 m, 742 vs, 639 m $cm^{-1}$. Far-IR (PE): 569 w, 551 w, 542 w, 442 w, 416 w, 362 w, 355 w, 200 m, 193 m, 180 m, 161 w, 75 w $cm^{-1}$. DTA/TG (Ar): 340 °C, calcd $M(NH_4[Tb(N_3C_{12}H_8)_4])$ = 84.5% of $M((NC_{12}H_8(NH)_2)[TbN_3C_{12}H_8)_4]$; measured, 87%; 390 °C, calcd M(C,Tb) = 74.6% of $M(NH_4[Tb(N_3C_{12}H_8)_4])$; measured, 76%.

**$(NC_{12}H_8(NH)_2)[Yb(N_3C_{12}H_8)_4]$ (3).** Yb (1.3 mmol = 235 mg) and 2-(2-pyridyl)-benzimidazole (1 mmol = 195 mg) were sealed in an evacuated Duran glass ampule and heated to 275 °C in 3 h. The reaction mixture was heated further to 315 °C in 1.5 h and cooled to 300 °C in 7 h and down to 240 °C in 100 h and to 150 °C within 100 h. It was then cooled to room temperature in another 72 h. Except for the excess Yb, the reaction was complete and gave transparent light yellow crystals of the product, which is air and moisture sensitive. Anal. Calcd $C_{60}H_{42}N_{15}Yb$: C, 62.96; N, 18.35; H, 3.67. Found: C, 63.10; N, 18.38; H, 3.78. MIR (KBr): 3080 w, 3042 m, 2920 w, 1601 s, 1565 m, 1511 m, 1474 m, 1455 s, 1441 s, 1422 s, 1374 s, 1330 s, 1294 m, 1278 s, 1269 s, 1250 m, 1148 m, 1108 w, 1072 w, 1050 w, 1005 m, 978 m, 815 m, 798 m, 745 vs, 640 m $cm^{-1}$. Far-IR (PE): 571 w, 550 w, 541 w, 474 vw, 436 w, 415 w, 358 w, 283 vw, 207 m sh, 202 m, 188 w, 151 w, 73 w $cm^{-1}$. DTA/TG (Ar): 320 °C, calcd $M(NH_4[Yb(N_3C_{12}H_8)_4])$ = 84.6% of $M((NC_{12}H_8(NH)_2)[YbN_3C_{12}H_8)_4]$; measured, 85%; 340 °C, calcd M(C,Yb) = 74.8% of $M(NH_4[Yb(N_3C_{12}H_8)_4])$; measured, 72%.

**$[La(N_3C_{12}H_8)_2(N_3C_{12}H_9)_2][La(N_3C_{12}H_8)_4](N_3C_{12}H_9)_2$ (4).** La (1 mmol = 139 mg) and 2-(2-pyridyl)-benzimidazole (2 mmol = 390 mg) together with Hg (0.25 mmol = 50 mg) were sealed in an evacuated Duran glass ampule and heated to 250 °C within 2.5 h. The reaction mixture was heated further to 330 °C in 2 h and the temperature held over 96 h. The reaction mixture was cooled to 200 °C in 300 h and then to room temperature within 20 h. Except for the excess La and Hg, the reaction was complete giving a microcrystalline sand-yellow product, which is air and moisture sensitive. Anal. Calcd $C_{120}H_{84}N_{30}La_2$: C, 64.83; N, 18.89; H, 3.78. Found: C, 64.74; N, 18.80; H, 3.85. MIR (KBr): 3080 w, 3049 m, 2923 w, 1597 vs, 1564 m, 1504 s, 1472 m, 1453 s, 1440 s, 1419 vs, 1374 vs, 1329 s, 1294 m, 1277 s, 1250 m, 1228 w, 1146 m, 1092 w, 1049 w, 1004 m, 976 m, 812 m, 799 m, 743 vs, 640 m $cm^{-1}$. Far-IR (PE): 569 w, 543 w, 513 w, 433 w, 409 w, 353 w, 282 vw, 276 vw, 205 m, 196 m, 176 m, 154 w, 72 w $cm^{-1}$. DTA/TG (Ar): 340 °C, calcd $M(NH_4[La(N_3C_{12}H_8)_4])$ = 84.1% of $M([La(N_3C_{12}H_8)_2(N_3C_{12}H_9)_2][La(N_3C_{12}H_8)_4](N_3C_{12}H_9)_2)$; measured, 84%; 395 °C, calcd M(C,La) = 73.9% of $M(NH_4[La(N_3C_{12}H_8)_4])$; measured, 67%.

**$[Sm(N_3C_{12}H_8)_2(N_3C_{12}H_9)_2][Sm(N_3C_{12}H_8)_4](N_3C_{12}H_9)_2$ (5).** Sm (1 mmol = 150 mg) and 2-(2-pyridyl)-benzimidazole (1 mmol = 195 mg) were sealed in an evacuated Duran glass ampule and heated to 270 °C in 9 h. This temperature was held for 7 days. The reaction mixture was then cooled to 200 °C in 77 h and to room temperature within 20 h. Except for the excess Sm, the reaction was complete, giving light yellow crystals of the product, which is air and moisture sensitive. Anal. Calcd $C_{120}H_{84}N_{30}Sm_2$: C, 64.23; N, 18.72; H, 3.74. Found: C, 63.79; N, 18.62; H, 3.78. MIR (KBr): 3079 w, 3042 m, 2921 w, 2853 w, 1599 vs, 1564 m, 1506 s, 1474 m, 1455 s, 1438 s, 1416 vs, 1371 s, 1328 s, 1274 s, 1147 m, 1092 w, 1051 w, 1007 m, 975 m, 814 m, 796 w, 745 vs, 640 m $cm^{-1}$. Far-IR (PE): 569 w, 546 w, 514 w, 433 w, 412 w, 355 m, 278 w, 208 m, 198 m, 179 w, 155 w $cm^{-1}$. Raman: 3082 m, 3064 m, 3052 m, 1598 vs, 1566 s, 1539 s, 1506 s, 1442 s, 1420 s, 1330 s, 1273 vs, 1142

(13) Müller-Buschbaum, K. *Z. Anorg. Allg. Chem*. **2002**, *628*, 2731−2737.

**Table 1.** Crystallographic Data for $(NC_{12}H_8(NH)_2)[Ln(N_3C_{12}H_8)_4]$, with Ln = Y (**1**), Yb (**3**), and $[Ln(N_3C_{12}H_8)_2(N_3C_{12}H_9)_2][Ln(N_3C_{12}H_8)_4](N_3C_{12}H_9)_2$, with Sm (**5**), Eu (**6**)[a]

| | **1** | **3** | **5** | **6** |
|---|---|---|---|---|
| formula | $C_{60}H_{42}N_{15}Y$ | $C_{60}H_{42}N_{15}Yb$ | $C_{120}H_{84}N_{30}Sm_2$ | $C_{120}H_{84}N_{30}Eu_2$ |
| fw | 1061.98 | 1145.11 | 2246.87 | 2250.06 |
| cryst syst | tetragonal | tetragonal | tetragonal | tetragonal |
| space group | $I4_1$ | $I4_1$ | $I4_1$ | $I4_1$ |
| $a = b$/pm | 1684.9(1) | 1683.03(7) | 1690.1(2) | 1685.89(9) |
| $c$/pm | 3735.0(3) | 3724.3(2) | 3759.5(4) | 3760.0(3) |
| $V$/($10^6$ pm$^3$) | 10603.5(14) | 10549.4(14) | 10739(2) | 10686.9(11) |
| $Z$ | 8 | 8 | 4 | 4 |
| $d_{calcd}$/(g cm$^{-1}$) | 1.328 | 1.441 | 1.387 | 1.396 |
| $\mu$/cm$^{-1}$ | 11.55 | 18.28 | 11.48 | 12.28 |
| $T$/K | 170(2) | 170(2) | 103(2) | 170(2) |
| data range | $3.42 \le 2\theta \le 52.0$ | $3.42 \le 2\theta \le 54.5$ | $2.64 \le 2\theta \le 52.48$ | $2.64 \le 2\theta \le 50.32$ |
| X-ray radiation | Mo K$\alpha$, $\lambda = 71.073$ | Mo K$\alpha$, $\lambda = 71.073$ | Mo K$\alpha$, $\lambda = 71.073$ | Mo K$\alpha$, $\lambda = 71.073$ |
| no. unique reflns | 10037 | 11670 | 9975 | 9283 |
| no. params | 684 | 688 | 687 | 687 |
| R1[b] for $n$ reflns with $F_o > 4\sigma(F_o)$; $n$ | 0.052; 5306 | 0.047; 8483 | 0.050; 4750 | 0.060; 6030 |
| R1 (all) | 0.127 | 0.068 | 0.118 | 0.098 |
| wR2[c] (all) | 0.101 | 0.129 | 0.117 | 0.138 |
| rem elec density/(e pm$^{-1}$) $\times 10^6$ | +0.37/−0.65 | +1.45/−1.18 | +0.69/−0.27 | +2.01/−1.08 |

[a] Deviations are given in parentheses. [b] $R1 = \sum[|F_o| - |F_c|]/\sum|F_o|$. [c] $wR2 = (\sum w(F_o^2 - F_c^2)^2)/(\sum w(F_o^4))^{1/2}$.[12]

m, 1117 w, 1006 vs, 990 m, 978 m, 854 w, 705 m, 628 m, 570 w, 207 w, 158 w, 135 m, 98 m cm$^{-1}$. DTA/TG (Ar): 350 °C, calcd $M(NH_4[Sm(N_3C_{12}H_8)_4]) = 84.3\%$ of $M([Sm(N_3C_{12}H_8)_2(N_3C_{12}H_9)_2][Sm(N_3C_{12}H_8)_4](N_3C_{12}H_9)_2)$; measured, 85%; 370 °C, calcd M(C,Sm) = 74.2% of $M(NH_4[Sm(N_3C_{12}H_8)_4])$; measured, 74%.

**$[Eu(N_3C_{12}H_8)_2(N_3C_{12}H_9)_2][Eu(N_3C_{12}H_8)_4](N_3C_{12}H_9)_2$ (6).** Eu (1 mmol = 152 mg) and 2-(2-pyridyl)-benzimidazole (1 mmol = 195 mg) together with Hg (0,25 mmol = 50 mg) were sealed in an evacuated Duran glass ampule and heated to 320 °C in 4.5 h. The reaction mixture was then cooled to 230 °C in 172 h and to 150 °C in 72 h. It was then cooled to room temperature within 7 h. Except for the Hg, the reaction mixture also showed excess Eu and unreacted pyridylbenzimidazole in addition to bright yellow crystals of the product, which is sensitive to air and moisture. Anal. Calcd $C_{120}H_{84}N_{30}Eu_2$: C, 64.14; N, 18.69; H, 3.73. Found: C, 64.83; N, 18.83; H, 3.84. MIR (KBr): 3056, 2963, 2923, 1772, 1597 vs, 1566 m, 1508 s, 1468 m, 1442 s, 1421 vs, 1406 s, 1372 vs, 1330 s, 1315 m, 1279 s, 1150 m, 1093 w, 1050 w, 1005 w, 973 m, 814 w, 797 w, 744 vs, 702 m, 640 m cm$^{-1}$. Far-IR (PE): 567 w, 542 w, 501 w, 431 w, 409 w, 355 w, 274 w, 209 sh w, 200 w, 182 w, 158 w cm$^{-1}$. DTA/TG (Ar): 310 °C, calcd $M(NH_4[Eu(N_3C_{12}H_8)_4]) = 84.4\%$ of $M([Eu(N_3C_{12}H_8)_2(N_3C_{12}H_9)_2][Eu(N_3C_{12}H_8)_4](N_3C_{12}H_9)_2)$; measured, 86%, 390 °C, calcd M(C,Eu) = 74.3% of $M(NH_4[Eu(N_3C_{12}H_8)_4])$; measured, 75%.

**X-ray Crystallographic Studies.** The best out of three single crystals of each of the compounds $(NC_{12}H_8(NH)_2)[Ln(N_3C_{12}H_8)_4]$, Ln = Y (**1**), Ln = Yb (**3**), and $[Ln(N_3C_{12}H_8)_2(N_3C_{12}H_9)_2][Ln(N_3C_{12}H_8)_4](N_3C_{12}H_9)_2$, Ln = Sm (**5**), Ln = Eu (**6**), were selected for single crystal X-ray investigations under glovebox conditions and sealed in glass capillaries. All data collections were carried out on a STOE IPDS-II diffractometer (Mo K$\alpha$ radiation, $\lambda$ = 0.7107 Å), for Ln = Sm at 103 K and for Ln = Y, Yb, and Eu at 170 K. For all four compounds, the structure was determined using direct methods.[14] All atoms were refined anisotropically by least-squares techniques.[15] Only some hydrogen positions were found from the differential Fourier card; the rest were calculated into preset positions adjusting their thermal parameters to 1.2 of the referring carbon atoms. Both $(NC_{12}H_8(NH)_2)[Ln(N_3C_{12}H_8)_4]$ with Ln = Y (**1**), Yb (**3**), and $[Ln(N_3C_{12}H_8)_2(N_3C_{12}H_9)_2][Ln(N_3C_{12}H_8)_4](N_3C_{12}H_9)_2$, Ln = Sm (**5**), Eu (**6**), are isotypic and crystallize in the tetragonal space group $I4_1$. The Eu, Y, and Yb compounds had to be refined as racemic twins while a reasonable Flack $x$ parameter of 0.04(23) was calculated for the Sm compound. Crystallographic data are summarized in Table 1. Further information was deposited at the Cambridge Crystallographic Data Centre, CCDC, 12 Union Road, Cambridge CB2 1EZ, U.K. (Fax: +44 1223336033. E-mail: deposit@ccdc.cam.ac.uk.) and may be requested by citing the deposition numbers CCDC-197287, 197288, 197289, and 197290, the name of the author, and the literature citation. The compounds **2** and **4** were investigated on powder samples in sealed capillaries on a STOE STADI P transmission diffractometer (Cu K$\alpha_1$ radiation $\lambda$ = 1.540598 Å, focused single-crystal germanium monochromator). The diffraction patterns of the La (**4**) and the Tb (**2**) compounds were compared with simulated diffractograms of **1**, **3**, **5,** and **6** and cell constants refined on 11 reflections with the best possible resolution for both **4** ($T$ = 293(2) K, $a$ = 1700.8(5) pm, $c$ = 3800(2) pm, $V$ = 10991.5(32) $\times$ $10^6$ pm$^3$) and **2** ($T$ = 293(2) K, $a$ = 1688(4) pm, $c$ = 3734(13) pm, $V$ = 10645(18) $\times$ $10^6$ pm$^3$).[16]

## Results and Discussion

**A. Formation of Homoleptic Pyridylbenzimidazolates of the Rare Earth Elements.** The reactions of lanthanide and group 3 metals with molten 2-(2-pyridyl)-benzimidazole can lead to three different groups of homoleptic pyridylbenzimidazolates of the rare earth elements. Which type of compound is formed depends mainly on the temperature of the melt as well as on the radius of the respective lanthanide. The groups $(NC_{12}H_8(NH)_2)[Ln(N_3C_{12}H_8)_4]$ and $[Ln(N_3C_{12}H_8)_2(N_3C_{12}H_9)_2][Ln(N_3C_{12}H_8)_4](N_3C_{12}H_9)_2$ presented here are formed first via a combined redox and acid−base autopro-

(14) Sheldrick, G. M. *SHELXS-86, Program for the resolution of Crystal Structures*; University of Göttingen: Göttingen, Germany, 1986.

(15) Sheldrick, G. M. *SHELXS-97, Program for the refinement of Crystal Structures*; University of Göttingen: Göttingen, Germany, 1997.

(16) *STOE & Cie GmbH WINXPOW V1.04, Program package for the operation of powder diffractometers and analysis of powder diffractograms*; Darmstadt, Germany, 1999.

tolysis reaction:

$$Ln + 5N_3C_{12}H_9 \xrightarrow{\text{melt}} (NC_{12}H_8(NH)_2)[Ln(N_3C_{12}H_8)_4] + {}^3/_2H_2 \quad (1)$$

$$2Ln + 10N_3C_{12}H_9 \xrightarrow{\text{melt}} [Ln(N_3C_{12}H_8)_2(N_3C_{12}H_9)_2][Ln(N_3C_{12}H_8)_4](N_3C_{12}H_9)_2 + 3H_2 \quad (2)$$

Compounds **1**−**3** refer to eq 1 whereas **4**−**6** refer to reaction 2.

Depending on the reactivity of the metal, a slight activation by producing a Hg amalgam first is necessary for most metals. Upon further heating, the compounds begin to decompose and form ammonium salts as another stable group of pyridylbenzimidazolates[13] as shown, e.g., for the pyridylbenzimidazolium salts:

$$(NC_{12}H_8(NH)_2)[Ln(N_3C_{12}H_8)_4] \xrightarrow{\text{melt, } \Delta T} NH_4[Ln(N_3C_{12}H_8)_4] + 2NH_3 + 12C \quad (3)$$

Upon further heating, the ammonium salts decompose, too,[13] giving additional carbon and ammonia as well as drops of the rare earth element (for details, see section C, describing thermal decompositions). Thus, characterization of compounds **1**−**6** and investigation of their thermal decomposition steps have resolved the question on how the ammonium pyridylbenzimidazolates are formed.[13] To confirm this, the temperatures derived for the formation of the ammonium salts from the DTA/TG measurements were transferred for direct syntheses having both the ammonium and the pyridylbenzimidazolium salts available and investigated on single crystals for ytterbium.

**B. Crystal Structure and Spectroscopic Investigations on $(NC_{12}H_8(NH)_2)[Ln(N_3C_{12}H_8)_4]$, with Ln = Y (1), Tb (2), Yb (3), and $[Ln(N_3C_{12}H_8)_2(N_3C_{12}H_9)_2][Ln(N_3C_{12}H_8)_4](N_3C_{12}H_9)_2$, with Ln = La (4), Sm (5), Eu (6).** To observe the differences between both types, single crystal X-ray investigations are necessary, while powder patterns are almost identical. The compounds **1**−**6** all crystallize isotypic in the tetragonal crystal system with space group $I4_1$. Like the ammonium salts $NH_4[Ln(N_3C_{12}H_8)_4]$,[13] the pyridylbenzimidazolium salts $(NC_{12}H_8(NH)_2)[Ln(N_3C_{12}H_8)_4]$ as well as $[Ln(N_3C_{12}H_8)_2(N_3C_{12}H_9)_2]^+$ containing salts are ionic with a cation/anion ratio of 1:1 (Figures 1 and 2). Anions and cations are monomeric, and the $[Ln(N_3C_{12}H_8)_4]^-$ anions strongly resemble each other in all salts including the ammonium salts. The rare earth atoms show an eightfold coordination of nitrogen atoms of four different pyridylbenzimidazolates giving distorted square antiprisms as coordination polyhedra. In addition, the compounds **4**−**6** show $[Ln(N_3C_{12}H_8)_2(N_3C_{12}H_9)_2]^+$ cations with a stronger distorted square antiprism as a coordination polyhedron formed of two pyridylbenzimidazolate anions and two neutral pyridylbenzimidazole molecules (Figure 3). In principle, this proves the common high coordination numbers of trivalent lanthanides, though it is rather high for homoleptic complexes with a pure nitrogen surrounding. A comparable coordination

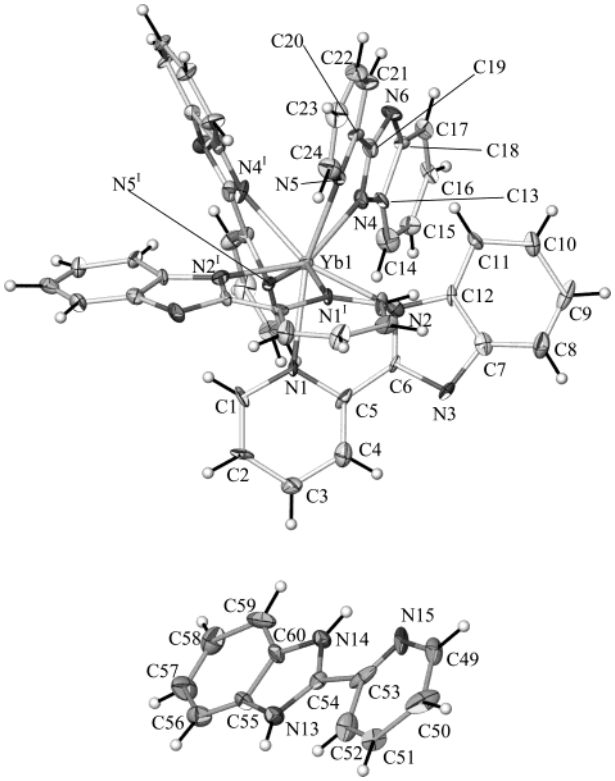


**Figure 1.** $[Yb(N_3C_{12}H_8)_4]^-$ and $(NC_{12}H_8(NH)_2)^+$ ions in $(NC_{12}H_8(NH)_2)[Yb(N_3C_{12}H_8)_4]$ (**3**) shown for Yb1. The thermal ellipsoids reflect 35% of the probability level of the atoms. Symmetry operation: I, $-x + 1$, $-y$, $z$.

is found for the porphyrinogen complexes of the lanthanides representing a remarkably stable sandwich structure of two ring systems known for different oxidation states of the lanthanides.[4−6,17−19] $[Sm(N\text{-}MeIm)_8]I_3$ exhibits a rather regular square antiprismatic coordination of eight N-Me-imidazole ligands around samarium, representing an exception because no geometry conditions of the ligand structure restrict the coordination.[20] The homoleptic dimeric toluene solvate $[Yb_2(Bu^t{}_2pz)_5]$ also shows an eightfold coordination of $Yb^{III}$ without a distinctive coordination polyhedron like the square antiprism, which is due to the structure and atom positions of the pyrazole ligand.[21] 2-(2-Pyridyl)-benzimidazole forms stable chelates by using only the two nitrogen atoms on one side of the ligand for Ln−N bonds. The third nitrogen atom does not coordinate the metal centers, thus giving monomeric anions and cations. Eightfold nitrogen coordination of rare earth elements is also found in homoleptic trivalent complexes with bis-[4,11-dihydro-5,7,12,14-tetramethyldibenzo-1,4,8,11-tetraazacyclotetradeca-1(14),5,7,12-tetraene],[22] showing sandwich structures such as the phthalocyanines. The 2,6-bis(benzimidazol-2-yl)pyridine com-

(17) Darovsky, A.; Keserashvili, V.; Harlow, R.; Mutikainen, I. *Acta Crystallogr.* **1994**, *B50*, 582−588.
(18) Janzcak, J.; Kubiak, R.; Jezierski, A. *Inorg. Chem.* **1999**, *38*, 2043−2049.
(19) Haghighi, M. S.; Rath, M.; Rotter, H. W.; Homborg, H. *Z. Anorg. Allg. Chem.* **1993**, *619*, 1887−1896.
(20) Evans, W. J.; Rabe, G. W.; Ziller, J. W. *Inorg. Chem.* **1994**, *33*, 3072−3078.
(21) Deacon, G. B.; Gitlits, A.; Skelton, B. W.; White, A. H. *J. Chem Soc., Chem. Commun.* **1999**, 1213−1214.
(22) Wang, Z.; Hu, N.; Sakata, K.; Hashimoto, M. *J. Chem. Soc., Dalton Trans.* **1999**, 1695−1700.

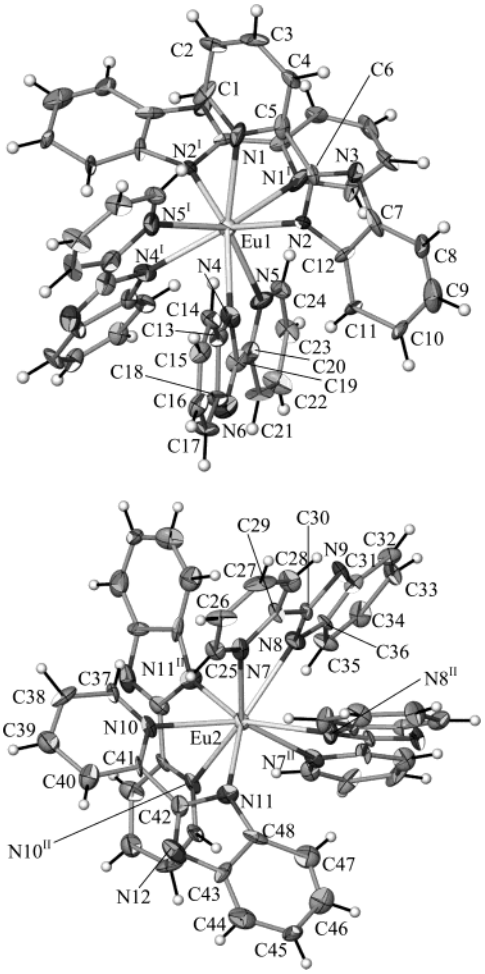


**Figure 2.** $[Eu(N_3C_{12}H_8)_4]^-$ and $[Eu(N_3C_{12}H_8)_2(N_3C_{12}H_9)_2]^+$ ions in $[Eu(N_3C_{12}H_8)_2(N_3C_{12}H_9)_2][Eu(N_3C_{12}H_8)_4](N_3C_{12}H_9)_2$ (**6**). The thermal ellipsoids reflect 35% of the probability level of the atoms. Symmetry operations: I, $-x + 1$, $-y$, $z$; II, $-x$, $-y + 1$, $z$.

plexes, containing the pyridylbenzimidazole fragment, too, exhibit a homoleptic character only in the presence of the weakly coordinating perchlorate ion[23] giving the high N-coordination number of nine.[12] This decreases in the comparable heteroleptic complexes[24,25] replacing nitrogen with oxygen atoms of the coordinating solvent or anions.

The pyridylbenzimidazolium−$Ln^{III}$−pyridylbenzimidazolates $(NC_{12}H_8(NH)_2)[Ln(N_3C_{12}H_8)_4]$ are formed with the smaller trivalent rare earth cations. The Ln−N distances vary with the size of the metal atom. As in the ammonium salts, four short amide metal bonds as well as four longer amine metal bonds are found. Table 2 contains selected distances and angles between atoms of **1**, **3**, **5**, and **6**. With $Y^{III}$ being almost the size of $Yb^{III}$,[26] **1** shows the shortest distances to nitrogen of 239(1)−258(2) pm, averaging 248 pm, which is close to the values found for $Yb^{III}$ in $NH_4[Yb(N_3C_{12}H_8)_4]$[13] that average 245 pm. The latter is in perfect accordance with $Yb^{III}$ in **3** with the shortest distances to nitrogen being in

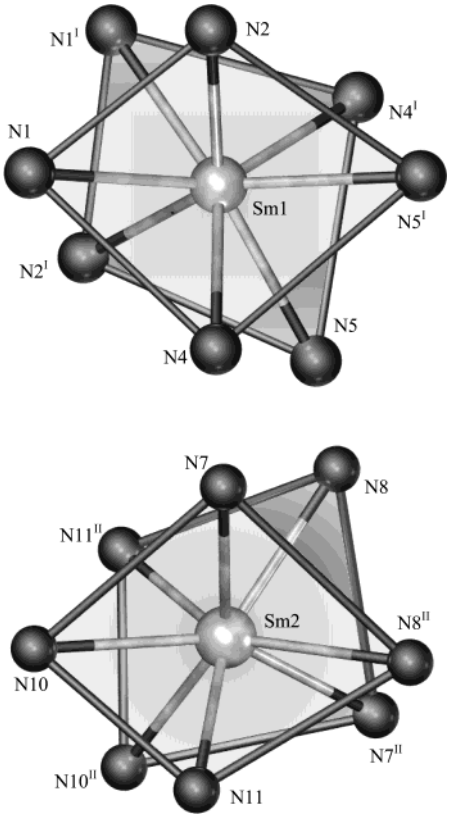


**Figure 3.** Distorted square antiprismatic coordination sphere of nitrogen atoms around the cationic samarium site in $[Sm(N_3C_{12}H_8)_2(N_3C_{12}H_9)_2][SmN_3C_{12}H_8)_4](N_3C_{12}H_9)_2$ (**5**). Lines between the nitrogen atoms are not bonds but show the distorted antiprism. The Sm atoms are depicted as large balls, the N atoms as small dark balls. Symmetry operations: I, $-x + 1$, $-y$, $z$; II, $-x$, $-y + 1$, $z$.

**Table 2.** Selected Distances (pm) and Angles (deg) between Atoms of $(NC_{12}H_8(NH)_2)[Ln(N_3C_{12}H_8)_4]$, with Ln = Y (**1**), Yb, (**3**), and $[Ln(N_3C_{12}H_8)_2(N_3C_{12}H_9)_2][Ln(N_3C_{12}H_8)_4](N_3C_{12}H_9)_2$, with Sm (**5**), Eu (**6**)[a]

| atoms | **1** | **3** | **5** | **6** |
|---|---|---|---|---|
| Ln1−N2 | 238(1) | 240(2) | 244(2) | 244(2) |
| Ln1−N4 | 243(1) | 244(1) | 246(2) | 246(2) |
| Ln1−N1 | 252(1) | 254(1) | 261(2) | 267(2) |
| Ln1−N5 | 256(1) | 252(1) | 265(2) | 260(2) |
| Ln2−N11 | 241.1(9) | 233(1) | 249(2) | 243(2) |
| Ln2−N8 | 247(1) | 241(1) | 258(2) | 261(2) |
| Ln2−N7 | 253(1) | 251(2) | 256(2) | 259(2) |
| Ln2−N10 | 255(1) | 246(2) | 260(2) | 255(2) |
| N1−Ln1−N2 | 67.8(4) | 69.9(4) | 66.8(6) | 65.7(6) |
| N4−Ln1−N5 | 66.0(4) | 66.8(4) | 62.9(6) | 65.2(6) |
| N7−Ln2−N8 | 66.3(4) | 66.9(4) | 66.5(6) | 64.7(6) |
| N10−Ln2−N11 | 66.9(4) | 65.8(5) | 65.6(6) | 65.7(5) |

[a] Deviations are given in parentheses.

the range 233(1)−254(1) pm, averaging 245 pm, too. The larger trivalent rare earth cations lead to the type $[Ln(N_3C_{12}H_8)_2(N_3C_{12}H_9)_2][Ln(N_3C_{12}H_8)_4](N_3C_{12}H_9)_2$. In addition to the anions being identical to the other salts, these compounds contain $[Ln(N_3C_{12}H_8)_2(N_3C_{12}H_9)_2]^+$ cations which exhibit only two short amide metal bonds and six longer amine metal bonds. The referring Sm−N distances in **5** range from 244(2) to 265(2) pm with an average of 255 pm. The longer distances match with the comparable amine $Sm^{III}$ bonds in the $[Sm(N\text{-}MeIm)_8]^{3+}$ cations (256−264 pm)[20] as well as with the heteroleptic complex $(MeCp)_2Sm(N\text{-}MeIm)_2$

(23) Wickleder, M. S. *Z. Anorg. Allg. Chem.* **1999**, *625*, 1556−1561.
(24) Piguet, C.; Williams, A. F.; Bernardinelli, G.; Moret, E.; Bünzli, J.-C. G. *Helv. Chim. Acta* **1992**, *75*, 1697−1717.
(25) Wang, S.; Zhu, Y.; Cui, Y.; Wang, L.; Luo, Q. *J. Chem. Soc., Dalton Trans.* **1994**, 2523−2530.
(26) Shannon, R. D. *Acta Crystallogr.* **1976**, *A32*, 751−767.

(262 and 267 pm).[27] The Eu−N distances in **6** range from 243(2) to 267(2) pm averaging 254 pm. The averages are closer to the upper limit because of the 2:6 ratio of Ln−N distances in the cations. Within the range of deviations, this is in good accordance and confirms the increase of ionic radii toward the light lanthanides such as $Nd^{III}$ in $NH_4[Nd(N_3C_{12}H_8)_4]$[13] with an average of 257 pm. Contrary to the ammonium salts, the ionic radii of the rare earth ions control whether the pyridylbenzimidazolium salts or the $[Ln(N_3C_{12}H_8)_2(N_3C_{12}H_9)_2]^+$ containing salts are obtained. Despite this difference, both types of compounds crystallize in the same structure type. The Ln−N distances are also in good accordance with other lanthanide amides such as pyrazolates for the shorter amide bonds,[10,11,20] or amine complexes such as bis-tris(*N*-*n*-propylbenzimidazol-2-ylmethyl)amine−$Eu^{III}$−triperchlorate for the longer amine bonds.[28]

In both groups of pyridylbenzimidazolates, the pyridyl-N species show the shortest Ln−N distances. The opposite is observed for 2,6-bis(benzimidazol-2-yl)pyridine complexes.[20] In these, the Ln−N-pyridyl distances are the longest. This is based on the different ligand structures, with the latter ligands having another benzimidazole side arm forming tridentate chelates instead of the bidentate pyridylbenzimidazolates. This geometrical restriction can be found in the chelate angles N1−Ln−N2, which are smaller in 2,6-bis(benzimidazol-2-yl)pyridine complexes[23−25] compared to **1** with N−Y−N angles of 65.8(4)−67.9(4)°, **3** with N−Yb−N angles of 65.8(5)−69.9(4)°, **5** with N−Sm−N anion angles of 63.0(6)−66.6(6)°, as well as N−Eu−N anion angles of 65.0(6)−66.5(6)° in **6**. Though the ammonium pyridylbenzimidazolates show identical values,[13] the square antiprisms are less distorted than in **1**−**6**. Thus, the anions exhibit a different shape with the pyridylbenzimidazolium salts looking much less regular and the $[Ln(N_3C_{12}H_8)_2(N_3C_{12}H_9)_2]^+$ cations being the most distorted (Figures 1−3). The lack of regularity of the square antiprismatic geometry can be evaluated by examining the angle between the eight Ln−N vectors and a potential eightfold inversion axis passing through the metal in a regular antiprism.[29] N-Me-imidazole ligands in $[Sm(N\text{-}MeIm)_8]I_3$,[20] which do not show any restrictions due to the ligand structure, exhibit a nearly regular square antiprism of eight N-MeIm ligands. The referring angle is very close to the ideal geometry (59.2°) with 57.8° and 57.6°.[20] In the ammonium pyridylbenzimidazolates,[13] the referring angles range already between 46.6° and 59.3°, while the type in **1**−**3** ranges from 37.8° to 67.2° for Yb in **3** and the most distorted type in **4**−**6** ranges from 37.0° to 68.7° for Sm in **5**. The reason for the different shape of the anions originates from the different cations. While the ammonium cation is almost like a ball and does not seem to have a distinct effect on the shape of the anion, the pyridylbenzimidazolium cation is a flat ring system that to some extent enforces further distortion of the anions. This effect is still visible in $[Ln(N_3C_{12}H_8)_2(N_3C_{12}H_9)_2][Ln(N_3C_{12}H_8)_4](N_3C_{12}H_9)_2$ (**4**−**6**), because it contains two unreacted pyridylbenzimidazole molecules and large cloudlike cations.

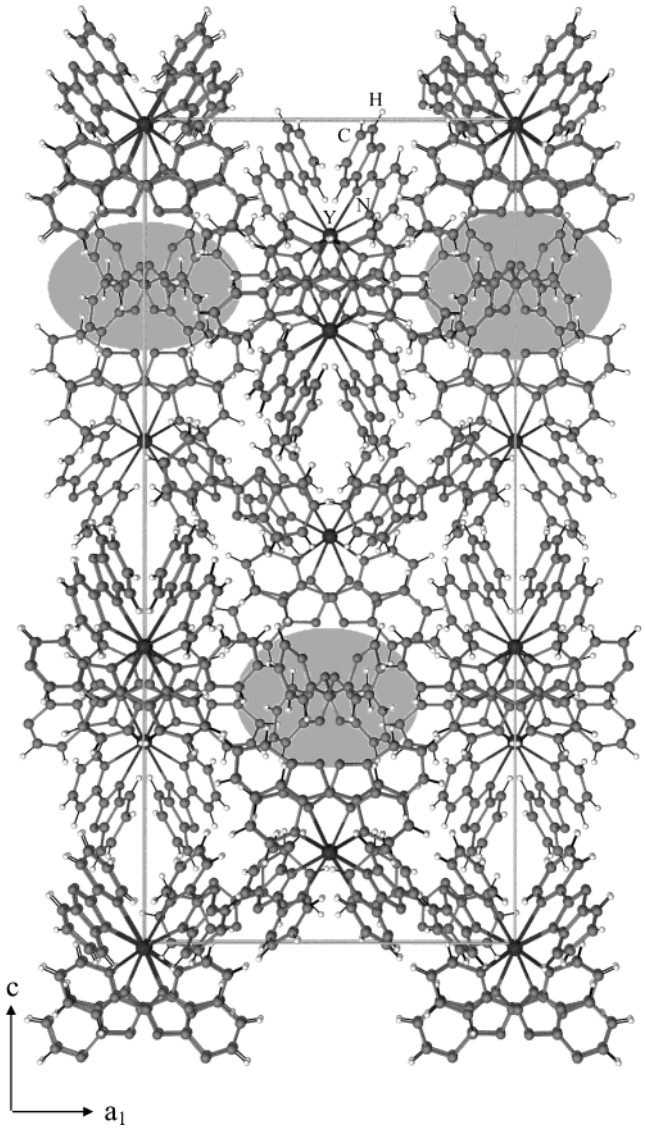


**Figure 4.** Crystal structure of $(NC_{12}H_8(NH)_2)[Y(N_3C_{12}H_8)_4]$ (**1**). The unit cell is shown along [010]. The positions of the cations in the structure are marked by shaded ellipsoids. Cations and anions are arranged in pairs. The Y atoms are depicted as large balls, the N atoms as light balls, and the C atoms as dark balls. The H atoms are depicted as small light balls. In the structure type $[Ln(N_3C_{12}H_8)_2(N_3C_{12}H_9)_2][Ln(N_3C_{12}H_8)_4](N_3C_{12}H_9)_2$, Ln = La, Sm, Eu (**4**−**6**), the shaded ellipsoids mark neutral ligand molecules. No pairs of ions are present as one type of the complex ions forms the cationic part of this structure.

The crystal structure of $(NC_{12}H_8(NH)_2)[Ln(N_3C_{12}H_8)_4]$ (**1**−**3**) is shown in Figure 4. Despite the differences in the Ln−N distances, the protonated species, and the distortion of the ions, the structure is similar to $[Ln(N_3C_{12}H_8)_2(N_3C_{12}H_9)_2][Ln(N_3C_{12}H_8)_4](N_3C_{12}H_9)_2$ (Figure 5). The structures of both types reflect the soft character of the ions causing the arrangement of anions and cations to be kept in both types, though this enforces an arrangement of pairs of certain anion and cation positions in the pyridylbenzimidazolium salts (**1**−**3**). The structures **1**−**3** as well as **4**−**6** can be deduced from a close packing of the ions. In both, anions and cations build complex sequences of tetragonal nets.

(27) Evans, W. J.; Rabe, G. W.; Ziller, J. W. *J. Organomet. Chem.* **1994**, *483*, 39−45.
(28) Su, C.-Y.; Kang, B.-S.; Liu, H.-Q.; Wang, Q.-G.; Chen, Z.-N.; Lu, Z.-L.; Tong, Y.-X.; Mak, T. C. W. *Inorg. Chem.* **1999**, *38*, 1374−1375.
(29) Hoard, J. L.; Silverton, J. V. *Inorg. Chem.* **1963**, *2*, 235−243.

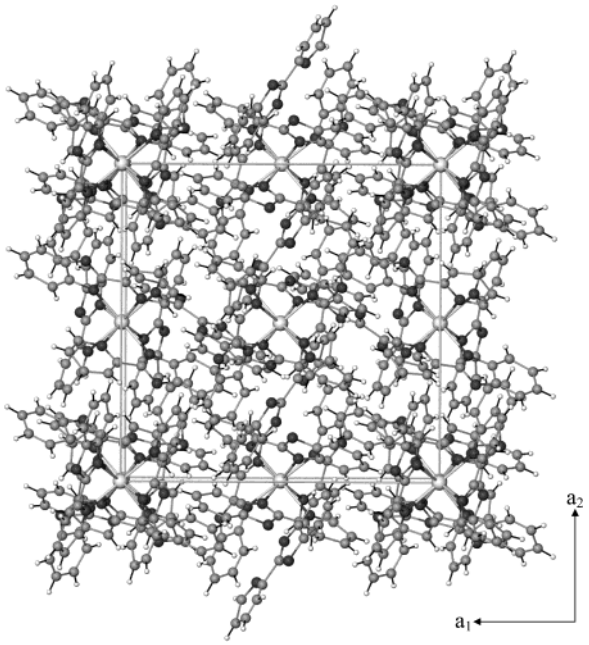


**Figure 5.** Crystal structure of $[Eu(N_3C_{12}H_8)_2(N_3C_{12}H_9)_2][Eu(N_3C_{12}H_8)_4](N_3C_{12}H_9)_2$ (**6**). The unit cell is shown along the tetragonal axis [001]. The Eu atoms are depicted as large light balls, the N atoms as dark balls, and the C atoms as gray balls. The H atoms are depicted as small light balls.

These nets form primitive packings of tetragonal sticks of anions and cations which center each other one-sided parallel to (001). Different sets of tetragonal sticks of the same ion type are shifted against each other along one of the *a*-axes. Due to the different distribution of charges, both types vary in the sequence of packing along the *c*-axis. This is different from the ammonium salts, which form cubic primitive packings of both anions and cations which center each other one-sided parallel to (010).

The pyridylbenzimidazolium salts $(NC_{12}H_8(NH)_2)[Ln(N_3C_{12}H_8)_4]$ (**1**−**3**) as well as the group $[Ln(N_3C_{12}H_8)_2(N_3C_{12}H_9)_2][Ln(N_3C_{12}H_8)_4](N_3C_{12}H_9)_2$ (**4**−**6**) were investigated spectroscopically with MIR and far-IR (and Raman for **5**) techniques. A comparison of the spectra with the bands of the free ligand shows a hypsochromic shift of several bands of about 10 wavenumbers: (2-(2-pyridyl)-benzimidazole IR 1592, 1487, 347 $cm^{-1}$; Raman 1489, 1316, 1262, 972 $cm^{-1}$).[13] This is in good accordance with the referring ammonium salts[13] and based on the nitrogen atoms coordinating the rare earth atoms. Though a certain splitting of bands (Yb (**3**): 1454 and 1442 $cm^{-1}$. IR, ligand: 1442 $cm^{-1}$. Yb (**3**): 1441 and 1435 $cm^{-1}$) as well as the additional IR band at 1420 $cm^{-1}$ is present in the pyridylbenzimidazolium salts, the latter not being observed for the ammonium salts $NH_4[Ln(N_3C_{12}H_8)_4]$, there is no distinct difference found for the spectra of the salts **4**−**6** (e.g., same splitting at least as shoulders observed for Sm (**5**): Raman, 1454 and 1442 $cm^{-1}$; IR, 1440 and 1434 $cm^{-1}$; Raman, ligand, 1449 $cm^{-1}$). Observation of intense bands comparable to other heterocycles[31] in the region 1500−1200 $cm^{-1}$ restricts this evidence further so that the presence of pyridylbenzimidazolium cations in $(NC_{12}H_8(NH)_2)[Ln(N_3C_{12}H_8)_4]$ cannot be unequivocally proven by MIR and Raman spectra.[30] Instead, the far-IR spectra of **1**−**6** offer a better possibility to distinguish between **1**−**3** and **4**−**6**. Both far-IR and Raman spectra show a series of bands that cannot be identified with the neutral ligand and represent the Ln−N stretching modes. For the group 3 metal Y (**1**), the far-IR bands are 243, 232, and 194 $cm^{-1}$, and they are thereby shifted in comparison to the respective bands of the lanthanides. For Tb (**2**), they are 200, 193, and 180 $cm^{-1}$, and for Yb (**3**), they are 207, 202, 188 $cm^{-1}$, whereas for La (**4**), 205, 196, 176 $cm^{-1}$, Sm (**5**) Raman 207 $cm^{-1}$, FIR 208, 198, 179 $cm^{-1}$, and Eu (**6**) FIR 209, 200, 182 $cm^{-1}$ are found. All are in the region of known Ln−N vibrations,[32,5,18] with a hypsochromic shift for each type. This corresponds to the expectations of the radii effect of the rare earth elements[33] and can be found for $NH_4[Ln(N_3C_{12}H_8)_4]$, too.[13] Due to the differences in the coordination spheres of compounds **1**−**3** compared to **4**−**6**, the hypsochromic shift cannot be observed throughout the lanthanide series but for each type separately, i.e., La to Eu as well as Tb to Yb. In addition, the ratio of intensities of those bands distinguishes both types of compounds. Therefore, the Tb compound (**2**) can be assumed to belong to the group corresponding to the smaller lanthanide radii while La belongs to the group $[Ln(N_3C_{12}H_8)_2(N_3C_{12}H_9)_2][Ln(N_3C_{12}H_8)_4](N_3C_{12}H_9)_2$, being the largest of the lanthanide cations.

**C. Thermal Decompositions of $(NC_{12}H_8(NH)_2)[Ln(N_3C_{12}H_8)_4]$, with Ln = Y (1), Tb (2), Yb (3), and $[Ln(N_3C_{12}H_8)_2(N_3C_{12}H_9)_2][Ln(N_3C_{12}H_8)_4](N_3C_{12}H_9)_2$, with Ln = La (4), Sm (5), Eu (6).** Simultaneous DTA and TG measurements were carried out in order to investigate the thermal behavior of the pyridylbenzimidazolium salts. Thereby the key information for understanding the formation of the ammonium salts $NH_4[Ln(N_3C_{12}H_8)_4]$[13] was collected (see later). The possibility to correlate the signals of the flow of warmth with the mass signals of the sample in context of the molecular masses of educts, products, and possible decomposition products as well as knowledge of educts and products provides the option to identify decomposition steps and thereby to understand the decomposition reactions.

The thermal decompositions of **1**−**6** show slight differences from the ammonium salts exhibiting two major decomposition steps instead of one.[13] While the formation reactions with yttrium (**1**), ytterbium (**3**), lanthanum (**4**), and samarium (**5**) were nearly complete, showing only a slight amount (max 2%) of unreacted pyridylbenzimidazole released at about 200 °C as the first DTA/TG signals, no volatile secondary products were released before. The reactions with terbium (**2**) and europium (**6**) gave about 10% and 62% unreacted ligand in the bulk indicating that the melt reactions to obtain (**2**) and (**6**) had yields of 90% and 38%, respectively, and also showed no volatile secondary products

(30) Colthup, N. B.; Daly, L. H.; Wiberley, S. E. *Introduction to Infrared and Raman Spectroscopy*, 2nd ed.; Academic Press; New York, 1975.
(31) Schrader, B. *Raman/Infrared Atlas of Organic Compounds*, 2nd ed.; Wiley VCH: New York, 1989.
(32) Weidlein, J.; Müller, U.; Dehnicke, K. *Schwingungsfrequenzen II, Nebengruppenelemente*; Georg Thieme Verlag: Stuttgart, New York, 1986.
(33) Nakamoto, K. *Infrared and Raman Spectra of Inorganic and Coordination Compounds*, 3rd ed.; Wiley VCH: New York, 1978.

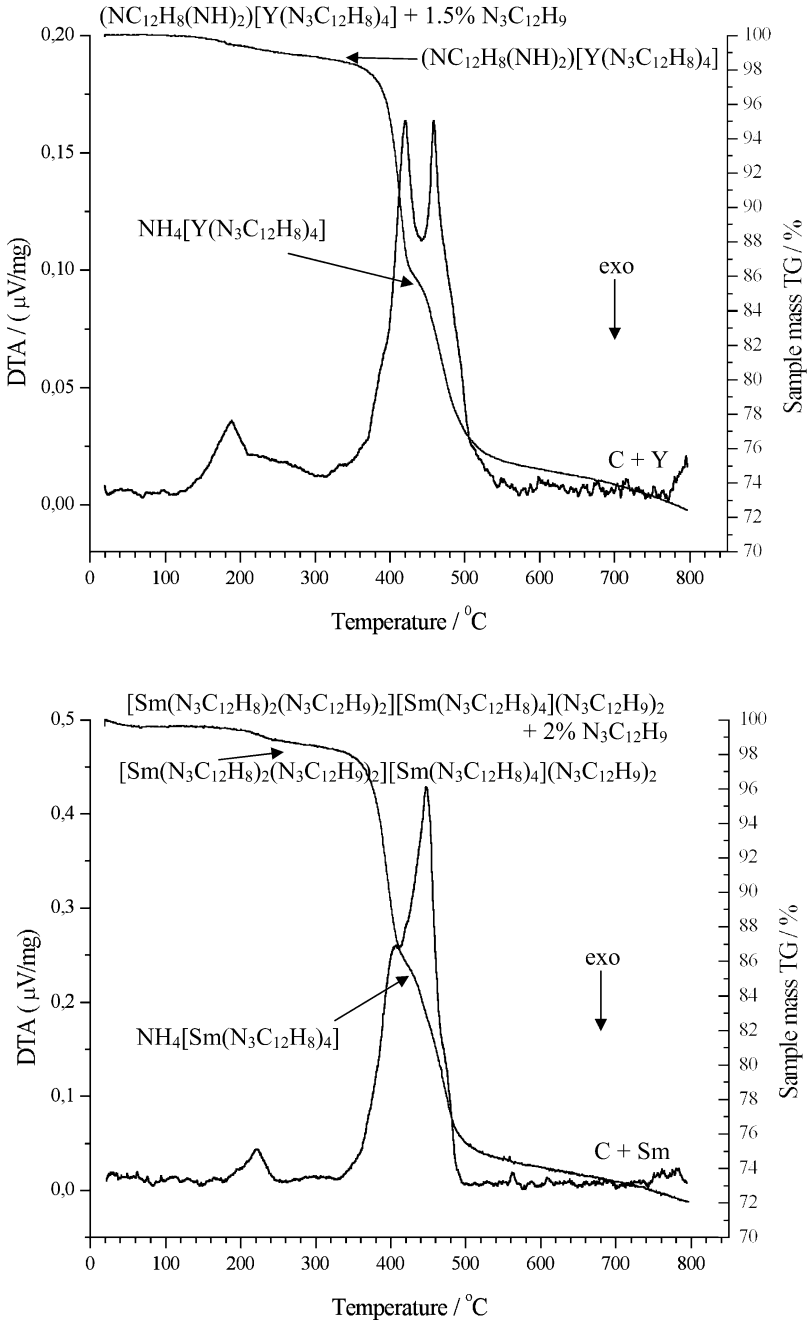


**Figure 6.** Thermal decomposition of $(NC_{12}H_8(NH)_2)[Y(N_3C_{12}H_8)_4]$ (**1**) (top) and $[Sm(N_3C_{12}H_8)_2(N_3C_{12}H_9)_2][Sm(N_3C_{12}H_8)_4](N_3C_{12}H_9)_2$ (**5**) (bottom) investigated with simultaneous DTA/TG in the temperature range 20−800 °C with a heating rate of 10 °C/min melt.

released before. All other reactions had yields beyond 90%. DTA/TG investigations on selected crystals did not show any phase released prior to the first decomposition step of the products. Yields of reactions in melts, if not a 100% phase pure product, cannot be easily determined by weighing giving a hard solid bulk product after cooling to room temperature. Instead, determination by thermal gravimetry offers a suitable alternative for these kinds of materials considering the chemically definite character of the melt reactions between rare earth metals and amines (see eqs 1 and 2 in section A, describing the formation of homoleptic pyridylbenzimidazolates). The problem of mechanically separating the bulk material is thereby avoided.

The compounds **1**−**6** decompose at varying temperatures without melting, in the first decomposition step giving ammonium salts as a stable intermediate of the decompositions and thus explaining the formation of ammonium salts as first known homoleptic pyridylbenzimidazolates: (Y (**1**), 350 °C, Tb (**2**), 340 °C, Yb (**3**), 320 °C, La (**4**), 340 °C, Sm (**5**), 350 °C, Eu (**6**), 310 °C). In a second decomposition step, the ammonium salts of all compounds (**1**−**6**) decompose, also at varying temperatures (Y (**1**), 430 °C, Tb (**2**), 390 °C, Yb (**3**), 340 °C, La (**4**), 395 °C, Sm (**5**), 370 °C, and Eu (**6**), 390 °C) (Figure 6). This second step is thereby identical to the decompositions of $NH_4[Ln(N_3C_{12}H_8)_4]$ (Ln = Nd, 410 °C; Yb, 340 °C).[13] In both decomposition steps, $NH_3$ is released, the residue in the first step consisting of some carbon and of $NH_4[Ln(N_3C_{12}H_8)_4]$ as well as of carbon

and the rare earth metal in the final step. The thermal decomposition investigations make it most likely that the unknown phase observed next to $NH_4[Nd(N_3C_{12}H_8)_4]$ and decomposing at 280 °C[13] was a phase of $Nd^{III}$ similar to compounds **1**−**3**. The DTA/TG investigations gave no evidence for a phase transition between **1**−**3** and **4**−**6**. All pyridylbenzimidazolates of the lanthanides and group 3 metals show a remarkable thermal stability as seen from the high decomposition temperatures. The ionic character of both groups of compounds must be taken into account for this behavior.

## Conclusion

The solid-state chemistry reaction route in the melt once again proved to be a suitable way to obtain homoleptic amides of the lanthanides in solvent free reactions.[13,21,34,35] This has also been transferred to group 3 metals with yttrium as well as to several other lanthanides. Formation of two new groups of pyridylbenzimidazolates (**1**−**3**, **4**−**6**) and investigations of their thermal decomposition show that the previously known ammonium pyridylbenzimidazolates of the lanthanides are thermal decomposition products of the salts presented here. Thereby the question on the formation of the ammonium salts was resolved and proven for ytterbium by single crystal X-ray investigations of both the ammonium and the pyridylbenzimidazolium salts. The combination of DTA and TG for simultaneous investigations can be used as a strong tool in this area of chemistry to gain information about phase purity of the products and thereby on yields as well as on the sequence of reactions and formation of decomposition products.[36]

**Acknowledgment.** We thank the Deutsche Forschungsgemeinschaft for supporting this work through the Graduiertenkolleg 549 “Azentrische Kristalle”.

**Supporting Information Available:** Tables of atomic coordinates, thermal parameters, bond distances and angles, and detailed crystallographic data for **1**−**6**. This material is available free of charge via the Internet at http://pubs.acs.org.

IC020681U

(34) Quitmann, C. C.; Müller-Buschbaum, K. *Z. Anorg. Allg. Chem.* **2002**, *628*, 2201.
(35) Müller-Buschbaum, K.; Quitmann, C. C. *Z. Kristallogr. Suppl.* **2002**, *19*, 47.
(36) Hemminger, W. F.; Cammenga, H. K. *Methoden der Thermischen Analyse*; Springer Verlag: New York, 1989.